Published in final edited form as:
Mech Ageing Dev. 2012 April ; 133(4): 176–185. doi:10.1016/j.mad.2012.01.008.

Retinoic acid-induced differentiation increases the rate of oxygen consumption and enhances the spare respiratory capacity of mitochondria in SH-SY5Y cells

Zhiyin Xun[a], **Do-Yup Lee**[a], **James Lim**[a], **Christie A. Canaria**[a], **Adam Barnebey**[a], **Steven M. Yanonne**[a], and **Cynthia T. McMurray**[a,b,c]

[a]Lawrence Berkeley National Laboratory, Life Sciences Division, 1 Cyclotron Rd., Berkeley, CA 94720 USA

[b]Department of Molecular Pharmacology and Experimental Therapeutics, Mayo Clinic and Foundation, 200 First St., Rochester, MN 55905 USA

[c]Department of Biochemistry and Molecular Biology, Mayo Clinic and Foundation, 200 First St., Rochester, MN 55905 USA

Abstract

Retinoic acid (RA) is used in differentiation therapy to treat a variety of cancers including neuroblastoma. The contributing factors for its therapeutic efficacy are poorly understood. However, mitochondria (MT) have been implicated as key effectors in RA-mediated differentiation process. Here we utilize the SH-SY5Y human neuroblastoma cell line as a model to examine how RA influences MT during the differentiation process. We find that RA confers an approximately 6-fold increase in the oxygen consumption rate while the rate of glycolysis modestly increases. RA treatment does not increase the number of MT or cause measurable changes in the composition of the electron transport chain. Rather, RA treatment significantly increases the mitochondrial spare respiratory capacity. We propose a competition model for the therapeutic effects of RA. Specifically, the high metabolic rate in differentiated cells limits the availability of metabolic nutrients for use by the undifferentiated cells and suppresses their growth. Thus, RA treatment provides a selective advantage for the differentiated state.

Keywords

Retinoic acid; neuroblastoma; glycolysis; oxidative phosphorylation

1. Introduction

Retinoic acid (RA), a metabolite of endogenous retinoids, induces differentiation in a variety of cells including skeletal myoblasts and neuroblasts (Mandili et al., 2011; Mankoo et al., 2010; Preis et al., 1988). Retinoids are related to vitamin A, and are used as a relatively new type of anti-cancer drug (alone or in combination) to treat skin cancer (Syed et al., 2009), cutaneous T-cell lymphoma (Zhang and Duvic, 2006) , acute promyelocytic leukemia (Sanz

To whom correspondence should be addressed: Cynthia T. McMurray, Lawrence Berkeley National Laboratory, Life Sciences Division, 1 Cyclotron Rd., Berkeley, CA 94720. Tel: (510)-486-6526; Fax: (510)-486-6880; ctmcmurray@lbl.gov.

et al., 2010), lung cancer (Kalemkerian et al., 1998), breast cancer (Levi et al., 2001; Naithani et al., 2008), ovarian cancer (Soprano et al., 2007), bladder cancer (El-Metwally and Hameed, 2008), kidney cancer (Motzer et al., 2000), head and neck cancer (Ahn et al., 1995), and neuroblastoma (Matthay et al., 1999). RA improves survival in patients with neuroblastoma, which is the most common extracranial solid pediatric tumor, and is responsible for approximately 15% of cancer deaths in children (Messi et al., 2008). In children with high-risk neuroblastoma, treatment with a retinoid called 13-cis-RA (isotretinoin) reduces the risk of recurrence after high-dose chemotherapy and stem cell transplantation (Matthay et al., 2009).

The contributing factors for the therapeutic effects of RA are poorly understood. Retinoids are essential for the maintenance of epithelial differentiation (Hansen et al., 2000). As such, they are likely to play a fundamental role in chemoprevention, at least in part, by attenuating cell growth. However, loss of cell division does not entirely account for the therapeutic effects of differentiation therapy. Neuroblastoma cells arise from immature neoplastic neural crest cells that possess properties of stem cells (Hogarty, 2003; Ross et al., 1995). *In vivo,* neuronal differentiation occurs continuously in neonates and young adults, yet, differentiation in the absence of RA treatment is insufficient to prevent neuroblastoma. Thus, RA treatment is likely to have additional effects that amplify its therapeutic potential.

The physiological consequences of RA treatment in neurons are difficult to dissect *in vivo*. However, a clonal human neuroblastoma cell line, SH-SY5Y, displays biochemical and electrophysiological properties similar to neurons (Hu et al., 2010; Oh-hashi et al., 1999). SH-SY5Y cells change their morphology and develop neurites upon treatment with RA (Kaur and Singh, 2007). During differentiation, SH-SY5Y cells begin to express neurofilaments, and opioid, muscarinic, and nerve growth factor receptors, all of which have been extensively characterized as neuronal markers (Ciccarone et al., 1989; Hu et al., 2010). Thus, SH-SY5Y cells provide a tool for probing molecular mechanisms of RA-mediated differentiation therapy.

In SH-SY5Y cells, at least three lines of evidence implicate mitochondria (MT) as key effectors of RA-induced differentiation, and poise them as important contributors to the therapeutic potential of RA *in vivo* (Hsieh et al., 2008; Ruff and Ong, 2000). First, RA is processed in the MT to some of its metabolically active forms (De Luca et al., 2000). Metabolic processing of retinoids involves two oxidation steps (Duester, 2008). The second oxidation step, retinal to retinoic acid, is an irreversible reaction that appears to occur through cytochrome P450 (CYP) (Napoli, 1999). CYP oxidizes RA often on the inner mitochondrial membrane (De Luca et al., 2000), and often form part of the multi-component electron transport chains (De Luca et al., 2000). Second, treatment with 9-cis RA induces RA receptor localization to MT, and induces expression of MT-associated genes (Everts and Berdanier, 2002). For instance, RA treatment induces rapid alterations in mRNA expression of cytochrome b-5, mitochondrial F0 complex subunit F6, cytochrome C oxidase subunit VIb (COX6B), and succinate dehydrogenase complex subunit C (Truckenmiller et al., 2001). Third, RA regulates gene expression directly through RA receptors α, β, and γ localized in MT (Everts and Berdanier, 2002) or indirectly via its influence on glucose flux (Huang et al., 1999). Taken together, these findings imply that the physiological consequences of RA treatment in SH-SY5Y cells are linked to MT, but their role remains enigmatic.

Here we utilized the SH-SY5Y cell line to elucidate the role of MT and the physiological effects of RA treatment in neuroblastoma cells. We find that RA induces a dramatic increase in the oxygen consumption rate in SH-SY5Y cells. RA treatment does not increase the number of MT or cause measurable changes in the composition of the electron transport

chain. Rather, RA increases mitochondrial spare respiratory capacity. We propose that RA treatment sequesters nutrients to support the high metabolic needs of the differentiated cells, thereby limiting the growth of the undifferentiated cells.

2. Materials and methods

2.1. Cell culture and differentiation

The human neuroblastoma cell line SH-SY5Y, obtained from ATCC (Manassas, VA, USA), was grown in a mixture of 1:1 Hyclone Minimum Essential Medium with Earle's Balanced Salts (MEM/EBSS) and Ham's F-12K Nutrient Medium supplemented with 10% FBS, 2 mM L-glutamine, 100 units/ml penicillin, and 100 μg/ml streptomycin. The cells were incubated at 37 ºC in 5% CO_2. The cell medium was replaced every 3 days and the cells were sub-cultured when they reached 85–90% confluence. Cells were differentiated as described previously (Encinas et al., 2000) with minor modifications. Briefly, cells were seeded at an initial cell density of 5×10^3 cells/cm^2. After 24 h of plating, cells were exposed to 10 μM *all-trans* RA (under which concentration we did not observe any noticeable cell death) in complete growth medium, as extensively documented previously (Cheung et al., 2009; Tosetti et al., 1998; Wang et al., 2006). The cells were maintained under these conditions for 5 days with medium change every two days. Subsequently, cells were washed three times with FBS-free growth medium to remove RA and then incubated with media containing 50 ng/ml recombinant human brain-derived neurotrophic factor (rhBDNF) in FBS-free growth medium for 5 days with medium change every two days. Cells were grown and differentiated in plastic petri dishes for phase contrast microscopy image acquisition, in XF96 cell culture microplates (Seahorse Bioscience, North Billerica, MA) for cellular metabolic flux analysis, in laminin pre-coated cover glasses for confocal microscopy analysis.

2.2. Cellular respiration assay

Oxygen consumption rate (OCR) and extracellular acidification rate (ECAR) were measured in real time using a Seahorse Bioscience XF96 extracellular flux analyzer (North Billerica, MA). After optimization of cell number, the desired number of cells was plated on XF96 cell culture microplates. Cells were seeded 20–24 hours before the metabolic flux analysis; undifferentiated cells were plated and treated with RA to induce differentiation. Plates were seeded at 3200 cells/well for differentiated cells at the initial stage of the differentiation process. On the day of extracellular flux analysis, cell growth medium was changed to XF assay media (pH 7.4, Seahorse Biosciences) supplemented with 25 mM glucose, 2 mM sodium pyruvate, and 2 mM glutaMAX using the XF Prep Station (Seahorse Bioscience). It is worth to note that we always supplemented with 2 mM sodium pyruvate for the XF flux analysis with the exception of the substrate titration experiments, in which the glucose- and pyruvate-free media was utilized. Cells were incubated for 1 h at 37 ºC without CO_2 prior to the cellular respiration measurement. The inhibitors of mitochondrial respiration, including oligomycin at 2 μg/ml, rotenone at 2 μM, carbonylcyanide p-trifluoromethoxyphenylhydrazone (FCCP) at 0.375 μM (an optimized concentration to give maximum respiratory capacity) or inhibitors of glycolysis, e.g., 2-deoxy-glucose (2-DG) at 100 mM, were auto-injected into the experimental wells after basal measurements and another three measurement cycles were performed. Each experimental point is an average of a minimum of three replicate wells and each experiment was performed at least three times with different plates. Immediately after finishing the flux measurements, cells were counted via a hemocytometer and/or Scepter 2.0 handheld automated cell counter (Millipore, Billerica, MA) and the values were used for normalization of OCR and ECAR values. All the XF96 data were reported as OCR or ECAR values normalized to cell counts or as percentage of baseline at the time point prior to compound injections.

2.3. MitoTracker labeling and confocal microscopy

MitoTracker Orange chloromethyltetramethylrosamine (CMTMRos) (Invitrogen, Carlsbad, CA) was used to label MT in live cells. Cells were labeled as instructed by the manufacturer. In short, cells were incubated in 100 nM of MitoTracker Orange in pre-warmed cell growth media for 20 min at 37 ºC. Staining solution was rinsed out thrice and replaced with fresh pre-warmed SH-SY5Y growth media prior to imaging. Images were acquired on a Zeiss LSM 710 inverted laser scanning confocal microscope. A 561-wavelength laser diode was used to excite MitoTracker Orange. The same laser settings (intensity, duration, scan speed) were utilized for all experiments pertaining to MitoTracker staining. Zen imaging software (Zeiss Inc.) was used for image acquisition, while FIJI, a processing package based on ImageJ (NIH), was used as the analysis software. Utilizing the polygon-tracing tool of FIJI, the outer edges of all cells were defined by a single user (to avoid variability) to calculate the surface areas. The generated 'cell-mask' from the bright-field image was then used to calculate the average MitoTracker signal for a given cell. A second region was selected to define the average background intensity level (a region devoid of cells and fluorescence signal), which was subsequently subtracted from the MitoTracker channel (background corrected). All measurements were then exported to Microsoft Excel for calculating the intensity per unit area.

2.4. Western blot analysis

Frozen cell pellets of equal cell numbers were thawed on ice and resuspended in 5X packed cell volume of Laemmli loading buffer (0.1 M Tris-HCl, pH 6.8, 20% glycerol, 4% sodium dodecyl sulfate, 0.02% bromophenol blue, and 0.1 M DTT) and sonicated with a Branson micro-tip Sonifier at 10% power for three 30 s bursts then heated to 95 ºC for 10 minutes. The denatured cell extracts were clarified by centrifugation at 14,000 RPM in an Eppendorf microfuge for 10 minutes. Proteins were resolved by appropriate SDS-PAGE gels of 7.5–12% depending on protein mass, transferred to 0.2 μm nitrocellulose, and blocked with 10% nonfat dried milk in 25 mM Tris (pH 7.4), 137 mM NaCl, 3 mM KCl, and 0.1% Tween-20 (TTBS/Milk) for 1 hour at room temperature. Immunoprobing was carried out with mouse monoclonal antibodies recognizing Complex I subunit NDUFB8 (1:2000 dilution) (Invitrogen), Complex II subunit A (1:10000 dilution) (Abcam), Complex III subunit Core 2 (1:1000 dilution) (Invitrogen), ATP synthase subunit beta (1:2000 dilution) (MitoSciences), rabbit monoclonal antibody recognizing Cytochrome C oxidase subunit II (1:5000 dilution) (Abcam), and mouse monoclonal antibody to alpha tubulin (1:5000 dilution) (Abcam) in TTBS/Milk. Western blots were visualized by ECL Plus chemiluminescence (GE Healthcare) and images captured with film and/or quantified using Versadoc imaging system and Quantity One software (Bio-Rad).

2.5. Statistical analysis

Values were expressed as average ± SD, unless otherwise stated. P-values were obtained from Student's t-test and were used to indicate significance. *, $p < 0.05$; **, $p < 0.01$.

3. Results

3.1. RA treatment reduces the dependence on glycolysis in SH-SY5Y human neuroblastoma cells

To evaluate the effects of RA treatment on mitochondrial metabolism, we exposed SH-SY5Y cells to RA, and followed changes in their morphology and proliferation with time. As expected, SH-SY5Y cells stopped proliferating after RA treatment, and underwent a dramatic morphological change, which was evident by 4 days in culture (Fig. 1A, B). RA-induced SH-SY5Y cells gradually developed mature neurites, which continued to develop throughout RA treatment. *In vivo*, neurites are maintained by growth factors. Thus, at 5 days

in culture, we added BDNF to the RA-treated cells. BDNF alone, does not induce differentiation of SH-SY5Y cells, but addition of the growth factor maintained healthy neurites of RA treated cells for up to one week (Fig. 1C-E). By 15 days in culture, RA and BDNF treatment resulted in striking cell aggregation and death of the differentiated cells (Fig. 1F). Based on these growth properties, we chose to measure the metabolic changes in SH-SY5Y cells treated for 5 days with RA followed by a 5-day exposure to BDNF. Under these conditions, the neurites were fully extended and measurable aggregation was absent in SH-SY5Y cells (Fig. 1D).

We tested whether RA altered the metabolism of SH-SY5Y cells. Glycolysis and oxidative phosphorylation are the two major energy-producing pathways in the cell, and the dependence of SH-SY5Y cells on each pathway was tested before and after RA treatment. In the first experiment, we blocked oxidative phosphorylation with the addition of oligomycin, an inhibitor of ATP synthase, and measured the rate of glycolysis. Glycolysis was measured as the extracellular acidification rate (ECAR) from lactic acid production before and after RA treatment. Lactic acid is formed from pyrvuate in the cytosol (Fig. 2). If energy production from oxidative phosphorylation is blocked and MT do not consume pyruvate, then glycolysis becomes the major source of pyruvate, which is converted to lactic acid (Fig. 2). Indeed, oligomycin treatment increased ECAR in both differentiated (D)-SH-SY5Y cells and undifferentiated (U)-SH-SY5Y cells (Fig. 3A), indicating that these cells increased their use of glycolysis in order to compensate for the loss of oxidative phosphorylation for energy production. The compensatory increase was more extensive for (D)-SH-SY5Y cells, however, indicating that loss of oxidative phosphorylation had a larger impact in the differentiated state (Fig. 3A).

As a complementary approach, we directly inhibited glycolysis by treating the cells with 2-deoxyglucose (2-DG), an analogue of glucose, and measured the effect on ECAR. Glucose hexokinase traps 2-DG in most cells, and blocks further glycolysis. Because ECAR is dominated by lactic acid production during glycolysis (Wu et al., 2007), we anticipated that 2-DG would decrease the rate of lactic acid production. Indeed, the addition of 2-DG resulted in a decrease of ECAR in both U-SH-SY5Y and D-SH-SY5Y cells (Fig. 3B), which are consistent with the oligomycin inhibition results. However, after addition of 2-DG, the ECAR decrease was more rapid and extensive in U-SH-SY5Y cells relative to D-SH-SY5Y cells (Fig. 3B). Specifically, the average ECAR at all time points after 2-DG addition decreased approximately 2-fold in U-SH-SY5Y cells relative to D-SH-SY5Y cells. Beyond 40 minutes, ECAR was low in both cultures, but U-SH-SY5Y remained approximately 40% lower than in D-SH-SY5Y cells. Collectively, the results indicated that U-SH-SY5Y cells depended more on glycolysis as an energy source relative to D-SH-SY5Y cells.

3.2. RA treatment preferentially enhances oxidative phosphorylation in SH-SY5Y cells

RA enters the MT and is oxidized by CYPs that form part of the multi-component electron transport chains on the mitochondrial inner membrane (De Luca et al., 2000). Thus, we tested whether RA-induced differentiation altered the oxidative phosphorylation capacity of MT. To address this issue, we evaluated whether the oxygen consumption rate (OCR) was altered in U-SH-SY5Y and D-SH-SY5Y cells. Actively respiring MT consume oxygen as ADP is converted into ATP. Thus, OCR correlates with the degree of oxidative phosphorylation and the activity of the electron transport chain.

OCR and ECAR were equivalent in U-SH-SY5Y cells. However, RA treatment induced a remarkable increase in mitochondrial metabolism in SH-SY5Y cells (Fig. 4A). Specifically, the OCR increased approximately 6-fold in D-SH-SY5Y relative to that in U-SH-SY5Y cells. Although D-SH-SY5Y cells increased their use of glycolysis, as judged by the increase in ECAR, the increase in the use of oxidative phosphorylation in D-SH-SY5Y cells

was substantially higher. Glucose is converted to pyruvate during glycolysis. Thus, the increase in OCR in D-SH-SY5Y cells might arise from enhanced glycolysis. To test this hypothesis, we provided D-SH-SY5Y cells and U-SH-SY5Y cells with pyruvate in the media to support OCR, but blocked glycolysis using 2-DG (Fig. 4B). Since pyruvate was available, addition of 2-DG had little effect on OCR in either cell type, but blocking glycolysis by addition of 2-DG did not alter the relative ratio of OCR between U-SH-SY5Y and D-SH-SY5Y cells (Fig. 4B). It was possible that the level of pyruvate was high enough to mask the contribution of glycolysis. However, OCR in D-SH-SY5Y cells remained 5-fold higher relative to U-SH-SY5Y after addition of oligomycin (Fig. 4B). Thus, RA treatment elevated both oxidative phosphorylation and glycolysis, but the elevated rate of glycolysis did not entirely account for the rise in OCR in D-SH-SY5Y cells.

3.3. The metabolic feature is an emergent property of RA-induced differentiation

We tested possible mechanisms for the RA-induced bioenergetic properties in D-SH-SY5Y cells. RA treatment might alter the substrate saturation level of the metabolic pathways. In the latter case, for example, U-SH-SY5Y and D-SH-SY5Y cells might have the same dependence on oxidative phosphorylation, but the intracellular level of pyruvate differentially saturated its use by MT in the two states. To test this possibility, we evaluated whether we could change the dependence on energy-production pathways by modulating the concentration of available substrates. In the first experiment, we supplemented glucose- and pyruvate-free media with pyruvate as an energy source, and measured the effects on oxidative phophorylation and glycolytic pathways by OCR and ECAR, respectively. Even at the lowest concentration of pyruvate (10^{-4} mM) and in the absence of glucose, OCR was high in D-SH-SY5Y cells (Fig. 5A), consistent with their use of oxidative phosphorylation for energy production. Increasing the pyruvate concentration 100-fold (to 0.01 mM) resulted in elevation of OCR approximately 2-fold, after which it reached saturation. ECAR in D-SH-SY5Y cells was low at any concentration of pyruvate, consistent with the finding that these cells depended less on glycolysis (Fig. 3). In contrast, U-SH-SY5Y cells efficiently used oxidative phophorylation if glucose was not available, but saturating levels of pyruvate did not increase the OCR or the ECAR to that observed in D-SH-SY5Y cells (Fig. 5A).

In the second analysis, we provided D-SH-SY5Y and U-SH-SY5Y cells with only glucose as a substrate (Fig. 5B). Under these conditions, ECAR rose significantly (2–3-fold) in D-SH-SY5Y cells compared to that with only pyruvate as a substrate, implying that these cells would use glycolysis as an energy source when the pyruvate level was low. However, at saturating glucose levels, OCR in D-SH-SY5Y cells remained significantly higher than ECAR, indicating that these cells maintained a greater dependence on oxidative phosphorylation for energy production. In U-SH-SY5Y cells, ECAR increased as a function of added glucose, while OCR decreased, consistent with a preference for the glycolytic pathway (Fig. 5B). However, saturating levels of glucose did not increase OCR and ECAR in these cells. Collectively, these data implied that availability of pyruvate and glucose substrates did not account for the elevated OCR observed in D-SH-SY5Y cells. Thus, the strong dependence on oxidative phosphorylation was an emergent property of D-SH-SY5Y cells specified by RA treatment, and did not depend on the availability of pyruvate and glucose, while U-SH-SY5Y cells were opportunistic and adapted their energy production according to the available substrates.

3.4. RA treatment does not increase mitochondrial number or substantially change the composition of the respiratory chain

RA enters the MT, where it is metabolized (De Luca et al., 2000). Thus, the elevated OCR in D-SH-SY5Y cells might also arise if the number or composition of MT changed in the differentiated cells. To measure the number of MT in D-SH-SY5Y and U-SH-SY5Y cells,

we stained them with MitoTracker Orange CM-H_2TMRos, a reduced derivative of dihydrotetramethylrosamine, which does not fluoresce until it is oxidized to CM-TMR in actively respiring cells (Jayaraman, 2005). We detected the number of MT by the overall fluorescence intensity in cells. We traced the outer edge of a cell to generate a 'cell-mask' from the bright-field image, and used the mask to calculate the average MitoTracker Orange signal for a given cell. RA treatment of SH-SY5Y cells induced morphological changes, resulting in neurite outgrowth as observed previously (Fig. 1). In the differentiated state, MT distributed throughout the neurites and in the cell body (Fig. 6A). Despite the increase in the cell surface areas (approximately threefold) in D-SH-SY5Y cells relative to that of U-SH-SY5Y cells, the average signal intensity of the undifferentiated (n = 226) and differentiated cells (n = 157) per unit area was similar (Fig. 6B). These results implied that cell morphology, but not the number of MT changed significantly upon differentiation of SH-SY5Y cells. In addition, accumulation of MitoTracker Orange CM-H_2TMRos in cells depends on the mitochondrial membrane potential (Deshmukh et al., 2000). Thus, that the average signal intensity was comparable between the RA treated and untreated cells also indicated that there was no significant difference in the average mitochondrial membrane potential between the undifferentiated and differentiated states.

To test whether RA treatment altered the composition of the electron transport chain within MT, we measured the expression of tubulin and key mitochondrial respiratory chain proteins in D-SH-SY5Y and U-SH-SY5Y cells. We analyzed the expression level of nuclear-encoded mitochondrial complex I subunit NDUFB8 (Davis et al., 2010), complex II subunit A (Gleason et al., 2011), complex III subunit core 2 (Suthammarak et al., 2010), and ATP synthase beta subunit (Howard et al., 2011), as well as MT-encoded complex IV subunit II (Pang et al., 2011) using specific antibodies (Fig. 6C). The expression levels were quantified and normalized to the tubulin loading control (Fig. 6D). We found that both mitochondrial- and nuclear-encoded proteins were expressed at similar levels before and after RA treatment (Fig. 6D). Thus, the increase in OCR resulting from the RA-induced differentiation was not due to measureable increases in mitochondrial number or composition of the electron transport chain.

3.5. RA treatment increases the spare respiratory capacity of MT

RA treatment did not appear to increase the number of MT or change the composition of the electron transport chain. Thus, we evaluated whether the increase in OCR after RA treatment altered the function of the MT or improved their efficiency. OCR is a combined measure of electron transport chain activity and proton leak (Dranka et al., 2010). As protein complexes in the inner membrane (NADH dehydrogenase, coenzyme Q-cytochrome c reductase, and cytochrome c oxidase) transfer electrons, the incremental release of energy along the chain is used to pump protons into the mitochondrial inter-membrane space (Fig. 2) (Stowe and Camara, 2009). Under some conditions, protons can re-enter the mitochondrial matrix without contributing to ATP synthesis. This process is known as proton leak (Voet et al., 2006). The energy dissipated by proton leak contributes to measureable OCR, but reduces the overall level of ATP production. Thus, we tested whether the RA-induced differentiation improved mitochondrial bioenergetics by reducing the proton leakage during respiration.

To measure proton leak, we inhibited ATP synthase at the last step of oxidative phosphorylation using oligomycin followed by treatment with rotenone, a mitochondrial complex I inhibitor. These inhibitors block ATP production at the last and the first step of the electron transport chain, respectively. While both oligomycin and rotenone block ATP production, rotenone prevents electron transport and the production of protons at NADH-Coenzyme Q Reductase (complex I). Thus, the difference in OCR between oligomycin and rotenone blocks is a measure of the proton leak. To directly compare the OCR between cells

that metabolize at different rates, we plotted OCR as a percent of baseline, and overlayed the plots of the differentiated and undifferentiated cells. Oligomycin inhibition in both U-SH-SY5Y and D-SH-SY5Y cells resulted in a drop in OCR, which did not change significantly after rotenone injection (Fig. 7A). Thus, blocking electron transport chain at the last step had a similar impact as blocking at the first step. These results suggested that the majority of OCR was driven by oxidative phosphorylation-coupled ATP production in both D-SH-SY5Y and U-SH-SY5Y cells (Fig. 7B). In both states, the contribution of proton leak was relatively small (around 15%, Fig. 7B). Thus, RA treatment did not improve MT function by reducing proton leak in D-SH-SY5Y cells relative to that in U-SH-SY5Y cells.

OCR in our experiments was measured in resting cells. However, MT have the ability to increase respiration and produce more energy as needed (Yadava and Nicholls, 2007). Thus, we tested whether RA treatment increased the efficiency of MT by increasing their reserve respiratory capacity, which is defined as the difference between the basal and maximum respiration for energy production through oxidative phosphorylation (Sansbury et al., 2011). To test this hypothesis, we blocked ATP synthase using oligomycin followed by addition of FCCP, an uncoupling agent that destroys both the proton gradient and the electrochemical potential in MT. FCCP allows for electron flow, but dissipates the proton gradient before it is used by ATP synthase, thereby blocking the conversion of ADP to ATP. Under these conditions, we measured OCR. The difference in OCR between the oligomycin inhibition before and after FCCP addition measures the degree to which MT are able to increase energy production in excess of their basal rates.

As before, addition of oligomycin resulted in a comparable decrease in their relative rate of oxygen consumption (Fig. 7C). Thus, in both D-SH-SY5Y and U-SH-SY5Y cells, MT were able to efficiently carry out oxidative phosphorylation despite their different relative OCR and ECAR. However, when oligomycin treatment was followed by addition of FCCP, we observed a substantial increase in OCR in D-SH-SY5Y cells (Fig. 7D). Thus, RA treatment improved the efficiency of MT after differentiation by increasing their capacity to utilize intracellular substrates.

4. Discussion

RA is used as a therapeutic treatment for cancers, yet the contributing factors for its therapeutic efficacy are poorly understood. Here we demonstrate that RA treatment elevates glycolysis and oxidative phosphorylation after differentiation of SH-SY5Y cells. The direct link between energy production pathway and the differentiation state poises mitochondrial metabolism as a key component of the therapeutic activity of RA treatment. The mRNA expression of MT-associated genes are altered upon RA treatment within 6 hours in SH-SY5Y cells (Truckenmiller et al., 2001), implying that changes on MT are required early in the differentiation process. At 5–14 days, when neurite extension is mature (Encinas et al., 2000), the protein content of the key components of the electron transport chain in MT is not significantly altered nor is the number of MT increased. However, we find that, at steady state, RA treatment fundamentally increases mitochondrial reserve capacity in the differentiated state (Fig. 7). These results suggest that enhancing mitochondrial bioenergetics is likely to contribute to the beneficial effects of RA.

The exact mechanism for how RA increases metabolism has yet to be resolved. RA stimulates both the activity and the mRNA expression level of glucokinase (Cabrera-Valladares et al., 2001; Fernandez-Mejia and Davidson, 1992), which catalyzes the conversion of glucose to glucose-6-phosphate. Thus, RA has the potential to increase glycolysis by either increasing the level of glucokinase or by increasing its activity (Cabrera-Valladares et al., 1999), resulting in an increase in pyruvate. However, we find that elevated

glycolysis does not entirely account for the rise in OCR in the differentiated state. Blocking glycolysis with 2-DG had little effect on the relative OCR between U-SH-SY5Y and D-SH-SY5Y cells (Fig. 4B). Thus, our results raise the possibility that the improvement in mitochondrial spare respiratory capacity after RA treatment relies, at least in part, on additional metabolic pathways. For example, acetyl-CoA is a substrate for mitochondrial metabolism and is used as starting materials for oxidative phosphorylation. Thus, RA-induced differentiation may increase OCR by increasing the level of alternative substrates, or by improving utilization of alternative metabolic pathways, such as fatty acid catabolism, to generate ATP, in addition to that generated by glycolysis.

Enhancement in mitochondrial reserve capacity has been observed in other systems (Perez et al., 2010). For example, in vascular smooth muscle cells, platelet-derived growth factor increases basal and maximal rates of glycolytic flux and mitochondrial oxygen consumption (Perez et al., 2010). Under these conditions, enhancement of these bioenergetic pathways leads to a substantial increase in the mitochondrial reserve capacity (Perez et al., 2010). The phosphatidylinositol 3-kinase (PI3K)/Akt pathway is required for the bioenergetic changes in the MT of vascular smooth muscle cells (Perez et al., 2010). Moreover, RA treatment activates the PI3K/Akt signaling pathway in SH-SY5Y cells (Chen et al., 2011), suggesting that PI3K/Akt may be at least one common pathway for the elevation of mitochondrial reserve capacity.

We propose a testable model in which the bioenergetic properties provide a basis for the therapeutic activity of RA. Neuroblastoma arises from undifferentiated neoplastic neural crest cells that possess properties of stem cells (Hu et al., 2010; Ohhashi et al., 1999; Ross et al., 1995). The ability of U-SH-SY5Y cells to use a glycolytic pathway provides a ready source of energy, and facilitates tumor growth. The undifferentiated cells have a low metabolic rate, but adapt their energy-production pathway according to the available substrates. Thus, their adaptability coupled with their low metabolism reduces their need for nutrients and provides a growth advantage. In contrast, RA treatment enhances the metabolic activity of neuroblastoma cells and heightens the demand for energy production through MT. Maintenance of differentiated cells takes precedence over tumor cell growth since differentiated and undifferentiated cells must compete for the same nutrients. At the same time, RA treatment enhances the reserve capacity of MT in differentiated cells. Thus, RA treatment provides a selective advantage for survival of differentiated cells and poises them to be suppressors of tumor growth.

While the therapeutic effects of RA treatment are complex, such a model is consistent with at least some clinical features of RA treatment in patients with neuroblastoma (Finklestein et al., 1992; Matthay et al., 1999). We find that RA treatment results in approximately 6-fold increase in the OCR relative to the same number of undifferentiated cells. The model predicts that the selective advantage of RA treatment would be limited by the ratio of tumor cells to differentiated cells. In this case, the most favorable outcome would occur when the tumor mass is small and the differentiated cell number is high. Indeed, RA therapy (in conjunction with other anti-cancer drugs) is most effective in children with smaller tumors, at a time when large numbers of their neurons are developing, and is relatively ineffective in adults with tumors and a fixed number of fully developed neurons (Finklestein et al., 1992). The model also predicts that the efficacy of RA will have an upper limit when the tumor mass exceeds the energy requirement of the surrounding differentiated neurons. Since differentiation would limit the therapeutic efficacy of RA treatment, the tumors would become resistant to RA therapy once neuronal differentiation had reached a maximum. Indeed, RA resistance has been observed (Finklestein et al., 1992; Freemantle et al., 2003; Reynolds et al., 1991). In fact, more than 50% of the patients with high-risk neuroblastoma treated with high dose RA after cytotoxic therapy have tumor recurrence (Reynolds et al.,

2000). Whatever the exact mechanism, the ability of RA treatment to increase the energy production in the MT provides a plausible mechanism for the therapeutic effects of RA, and poises RA as a metabolic regulator of tumor growth. These results indicate that cellular bioenergetics may be a common mechanism that links the beneficial effects of RA among diverse cancers, and provides insight into the molecular mechanism for differentiation therapy.

Acknowledgments

This work was supported by the Mayo Foundation, the National Institutes of Health grants NS069177 (CTM and TRN), NS40738 (CTM), NS062384 (CTM), and NS060115 (CTM).

Abbreviations

RA	retinoic acid
MT	mitochondria
CYP	cytochorme P450
OCR	oxygen consumption rate
ECAR	extracellular acidification rate
FCCP	carbonylcyanide p-trifluoromethoxyphenylhydrazone
2-DG	2-deoxy-glucose
D	differentiated
U	undifferentiated

References

Ahn MJ, Langenfeld J, Moasser MM, Rusch V, Dmitrovsky E. Growth suppression of transformed human bronchial epithelial cells by all-trans-retinoic acid occurs through specific retinoid receptors. Oncogene. 1995; 11:2357–2364. [PubMed: 8570187]

Cabrera-Valladares G, German MS, Matschinsky FM, Wang J, Fernandez-Mejia C. Effect of retinoic acid on glucokinase activity and gene expression and on insulin secretion in primary cultures of pancreatic islets. Endocrinology. 1999; 140:3091–6. [PubMed: 10385401]

Cabrera-Valladares G, Matschinsky FM, Wang J, Fernandez-Mejia C. Effect of retinoic acid on glucokinase activity and gene expression in neonatal and adult cultured hepatocytes. Life Sciences. 2001; 68:2813–24. [PubMed: 11432447]

Chen K-F, Chen H-L, Tai W-T, Feng W-C, Hsu C-H, Chen P-J, Cheng A-L. Activation of Phosphatidylinositol 3-Kinase/Akt Signaling Pathway Mediates Acquired Resistance to Sorafenib in Hepatocellular Carcinoma Cells. Journal of Pharmacology and Experimental Therapeutics. 2011; 337:155–161. [PubMed: 21205925]

Cheung YT, Lau WK, Yu MS, Lai CS, Yeung SC, So KF, Chang RC. Effects of all-trans-retinoic acid on human SH-SY5Y neuroblastoma as in vitro model in neurotoxicity research. Neurotoxicology. 2009; 30:127–35. [PubMed: 19056420]

Ciccarone V, Spengler BA, Meyers MB, Biedler JL, Ross RA. Phenotypic Diversification in Human Neuroblastoma Cells: Expression of Distinct Neural Crest Lineages. Cancer Research. 1989; 49:219–225. [PubMed: 2535691]

Davis CW, Hawkins BJ, Ramasamy S, Irrinki KM, Cameron BA, Islam K, Daswani VP, Doonan PJ, Manevich Y, Madesh M. Nitration of the mitochondrial complex I subunit NDUFB8 elicits RIP1- and RIP3-mediated necrosis. Free Radic Biol Med. 2010; 48:306–17. [PubMed: 19897030]

De Luca LM, Hansen LA, Sigman CC, Andreola F, Ross SA, Kelloff GJ. Retinoids in chemoprevention and differentiation therapy. Carcinogenesis. 2000; 21:1271–1279. [PubMed: 10874003]

Deshmukh M, Kuida K, Johnson EM Jr. Caspase inhibition extends the commitment to neuronal death beyond cytochrome c release to the point of mitochondrial depolarization. Journal of Cell Biology. 2000; 150:131–43. [PubMed: 10893262]

Dranka BP, Hill BG, Darley-Usmar VM. Mitochondrial reserve capacity in endothelial cells: The impact of nitric oxide and reactive oxygen species. Free Radic Biol Med. 2010; 48:905–14. [PubMed: 20093177]

Duester G. Retinoic acid synthesis and signaling during early organogenesis. Cell. 2008; 134:921–31. [PubMed: 18805086]

El-Metwally TH, Hameed DA. The effectiveness of retinoic acid treatment in bladder cancer - Impact on recurrence, survival and TGF alpha and VEGF as end-point biomarkers. Cancer Biology & Therapy. 2008; 7:92–100. [PubMed: 18347417]

Encinas M, Iglesias M, Liu Y, Wang H, Muhaisen A, Cena V, Gallego C, Comella JX. Sequential treatment of SH-SY5Y cells with retinoic acid and brain-derived neurotrophic factor gives rise to fully differentiated, neurotrophic factor-dependent, human neuron-like cells. Journal of Neurochemistry. 2000; 75:991–1003. [PubMed: 10936180]

Everts HB, Berdanier CD. Regulation of mitochondrial gene expression by retinoids. IUBMB Life. 2002; 54:45–9. [PubMed: 12440518]

Fernandez-Mejia C, Davidson MB. Regulation of glucokinase and proinsulin gene expression and insulin secretion in RIN-m5F cells by dexamethasone, retinoic acid, and thyroid hormone. Endocrinology. 1992; 130:1660–8. [PubMed: 1537314]

Finklestein JZ, Krailo MD, Lenarsky C, Ladisch S, Blair GK, Reynolds CP, Sitarz AL, Hammond GD. 13-cis-retinoic acid (NSC 122758) in the treatment of children with metastatic neuroblastoma unresponsive to conventional chemotherapy: report from the Childrens Cancer Study Group. Medical and pediatric oncology. 1992; 20:307–311. [PubMed: 1608352]

Freemantle SJ, Spinella MJ, Dmitrovsky E. Retinoids in cancer therapy and chemoprevention: promise meets resistance. Oncogene. 2003; 22:7305–7315. [PubMed: 14576840]

Gleason C, Huang S, Thatcher LF, Foley RC, Anderson CR, Carroll AJ, Millar AH, Singh KB. Mitochondrial complex II has a key role in mitochondrial-derived reactive oxygen species influence on plant stress gene regulation and defense. Proceedings of the National Academy of Sciences of the United States of America. 2011; 108:10768–10773. [PubMed: 21670306]

Hansen LA, Sigman CC, Andreola F, Ross SA, Kelloff GJ, De Luca LM. Retinoids in chemoprevention and differentiation therapy. Carcinogenesis. 2000; 21:1271–9. [PubMed: 10874003]

Hogarty MD. The requirement for evasion of programmed cell death in neuroblastomas with MYCN amplification. Cancer Lett. 2003; 197:173–9. [PubMed: 12880978]

Howard AD, Verghese PB, Arrese EL, Soulages JL. The beta-subunit of ATP synthase is involved in cellular uptake and resecretion of apoA-I but does not control apoA-I-induced lipid efflux in adipocytes. Molecular and Cellular Biochemistry. 2011; 348:155–64. [PubMed: 21069432]

Hsieh RH, Lin YW, Lien LM, Yeh TS, Wu HM, Liu YL. 9-cis retinoic acid induces retinoid X receptor localized to the mitochondria for mediation of mitochondrial transcription. Biochemical and Biophysical Research Communications. 2008; 377:351–354. [PubMed: 18840407]

Hu LS, Xie HR, Li GY. SH-SY5Y human neuroblastoma cell line: in vitro cell model of dopaminergic neurons in Parkinson's disease. Chinese Medical Journal. 2010; 123:1086–1092. [PubMed: 20497720]

Huang X, Eriksson KF, Vaag A, Lehtovirta M, Hansson M, Laurila E, Kanninen T, Olesen BT, Kurucz I, Koranyi L, Groop L. Insulin-regulated mitochondrial gene expression is associated with glucose flux in human skeletal muscle. Diabetes. 1999; 48:1508–1514. [PubMed: 10426366]

Jayaraman S. Flow cytometric determination of mitochondrial membrane potential changes during apoptosis of T lymphocytic and pancreatic beta cell lines: comparison of tetramethylrhodamineethylester (TMRE), chloromethyl-X-rosamine (H2-CMX-Ros) and

MitoTracker Red 580 (MTR580). Journal of Immunological Methods. 2005; 306:68–79. [PubMed: 16256133]

Kalemkerian GP, Jiroutek M, Ettinger DS, Dorighi JA, Johnson DH, Mabry M. A phase II study of all-trans-retinoic acid plus cisplatin and etoposide in patients with extensive stage small cell lung carcinoma: an Eastern Cooperative Oncology Group Study. Cancer. 1998; 83:1102–8. [PubMed: 9740074]

Kaur G, Singh J. Transcriptional regulation of polysialylated neural cell adhesion molecule expression by NMDA receptor activation in retinoic acid-differentiated SH-SY5Y neuroblastoma cultures. Brain Research. 2007; 1154:8–21. [PubMed: 17499225]

Levi MS, Borne RF, Williamson JS. A review of cancer chemopreventive agents. Current Medicinal Chemistry. 2001; 8:1349–62. [PubMed: 11562271]

Mandili G, Marini C, Carta F, Zanini C, Prato M, Khadjavi A, Turrini F, Giribaldi G. Identification of phosphoproteins as possible differentiation markers in all-trans-retinoic acid-treated neuroblastoma cells. PLoS One. 2011; 6:e18254. [PubMed: 21573212]

Mankoo BS, Reijntjes S, Francis-West P. Retinoic acid is both necessary for and inhibits myogenic commitment and differentiation in the chick limb. International Journal of Developmental Biology. 2010; 54:125–134. [PubMed: 19757389]

Matthay KK, Reynolds CP, Seeger RC, Shimada H, Adkins ES, Haas-Kogan D, Gerbing RB, London WB, Villablanca JG. Long-term results for children with high-risk neuroblastoma treated on a randomized trial of myeloablative therapy followed by 13-cis-retinoic acid: a children's oncology group study. J Clin Oncol. 2009; 27:1007–13. [PubMed: 19171716]

Matthay KK, Villablanca JG, Seeger RC, Stram DO, Harris RE, Ramsay NK, Swift P, Shimada H, Black CT, Brodeur GM, Gerbing RB, Reynolds CP. Treatment of high-risk neuroblastoma with intensive chemotherapy, radiotherapy, autologous bone marrow transplantation, and 13-cis-retinoic acid. Children's Cancer Group. New England Journal of Medicine. 1999; 341:1165–73.

Messi E, Florian MC, Caccia C, Zanisi M, Maggi R. Retinoic acid reduces human neuroblastoma cell migration and invasiveness: effects on DCX, LISI, neurofilaments-68 and vimentin expression. Bmc Cancer. 2008; 8

Motzer RJ, Murphy BA, Bacik J, Schwartz LH, Nanus DM, Mariani T, Loehrer P, Wilding G, Fairclough DL, Cella D, Mazumdar M. Phase III trial of interferon alfa-2a with or without 13-cis-retinoic acid for patients with advanced renal cell carcinoma. Journal of Clinical Oncology. 2000; 18:2972–2980. [PubMed: 10944130]

Naithani R, Huma LC, Moriarty RM, McCormick DL, Mehta RG. Comprehensive review of cancer chemopreventive agents evaluated in experimental carcinogenesis models and clinical trials. Current Medicinal Chemistry. 2008; 15:1044–71. [PubMed: 18473802]

Napoli JL. Interactions of retinoid binding proteins and enzymes in retinoid metabolism. Biochimica et Biophysica Acta. 1999; 1440:139–62. [PubMed: 10521699]

Oh-hashi K, Maruyama W, Yi H, Takahashi T, Naoi M, Isobe K. Mitogen-activated protein kinase pathway mediates peroxynitrite-induced apoptosis in human dopaminergic neuroblastoma SH-SY5Y cells. Biochemical and Biophysical Research Communications. 1999; 263:504–9. [PubMed: 10491322]

Pang L, Qiu T, Cao X, Wan M. Apoptotic role of TGF-beta mediated by Smad4 mitochondria translocation and cytochrome c oxidase subunit II interaction. Experimental Cell Research. 2011; 317:1608–20. [PubMed: 21324314]

Perez J, Hill BG, Benavides GA, Dranka BP, Darley-Usmar VM. Role of cellular bioenergetics in smooth muscle cell proliferation induced by platelet-derived growth factor. Biochemical Journal. 2010; 428:255–267. [PubMed: 20331438]

Preis PN, Saya H, Nádasdi L, Hochhaus G, Levin V, Sadée W. Neuronal Cell Differentiation of Human Neuroblastoma Cells by Retinoic Acid plus Herbimycin A. Cancer Research. 1988; 48:6530–6534. [PubMed: 2846152]

Reynolds CP, Kane DJ, Einhorn PA, Matthay KK, Crouse VL, Wilbur JR, Shurin SB, Seeger RC. Response of neuroblastoma to retinoic acid in vitro and in vivo. Progress in Clinical and Biological Research. 1991; 366:203–11. [PubMed: 2068138]

Reynolds CP, Wang Y, Melton LJ, Einhorn PA, Slamon DJ, Maurer BJ. Retinoic-acid-resistant neuroblastoma cell lines show altered MYC regulation and high sensitivity to fenretinide. Medical and pediatric oncology. 2000; 35:597–602. [PubMed: 11107126]

Ross R, Spengler B, Domenech C, Porubcin M, Rettig W, Biedler J. Human neuroblastoma I-type cells are malignant neural crest stem cells. Cell Growth Differ. 1995; 6:449–456. [PubMed: 7794812]

Ruff SJ, Ong DE. Cellular retinoic acid binding protein is associated with mitochondria. FEBS Letters. 2000; 487:282–6. [PubMed: 11150525]

Sansbury BE, Jones SP, Riggs DW, Darley-Usmar VM, Hill BG. Bioenergetic function in cardiovascular cells: the importance of the reserve capacity and its biological regulation. Chem Biol Interact. 2011; 191:288–95. [PubMed: 21147079]

Sanz MA, Montesinos P, Rayon C, Holowiecka A, de la Serna J, Milone G, de Lisa E, Brunet S, Rubio V, Ribera JM, Rivas C, Krsnik I, Bergua J, Gonzalez J, Diaz-Mediavilla J, Rojas R, Manso F, Ossenkoppele G, Gonzalez JD, Lowenberg B. Risk-adapted treatment of acute promyelocytic leukemia based on all-trans retinoic acid and anthracycline with addition of cytarabine in consolidation therapy for high-risk patients: further improvements in treatment outcome. Blood. 2010; 115:5137–46. [PubMed: 20393132]

Soprano DR, Ravikumar S, Perez-Liz G, Del Vale L, Soprano KJ. Insulin receptor substrate-1 is an important mediator of ovarian cancer cell growth suppression by all-trans retinoic acid. Cancer Research. 2007; 67:9266–9275. [PubMed: 17909034]

Stowe DF, Camara AK. Mitochondrial reactive oxygen species production in excitable cells: modulators of mitochondrial and cell function. Antioxid Redox Signal. 2009; 11:1373–414. [PubMed: 19187004]

Suthammarak W, Morgan PG, Sedensky MM. Mutations in mitochondrial complex III uniquely affect complex I in Caenorhabditis elegans. Journal of Biological Chemistry. 2010; 285:40724–31. [PubMed: 20971856]

Syed Z, Cheepala SB, Gill JN, Stein J, Nathan C, Digiovanni J, Batra V, Adegboyega P, Kleiner HE, Clifford JL. All-trans retinoic acid suppresses Stat3 signaling during skin carcinogenesis. Cancer Prevention Research. 2009; 2:903–11. [PubMed: 19789299]

Tosetti P, Taglietti V, Toselli M. Functional changes in potassium conductances of the human neuroblastoma cell line SH-SY5Y during in vitro differentiation. Journal of Neurophysiology. 1998; 79:648–58. [PubMed: 9463428]

Truckenmiller ME, Marquis PV, Chris C, Mark C, David MD, William JF, Kevin GB. Gene expression profile in early stage of retinoic acid-induced differentiation of human SH-SY5Y neuroblastoma cells. Restorative Neurology and Neuroscience. 2001; 18:67–80. [PubMed: 11847429]

Voet, D.; Voet, JG.; Pratt, CW. Fundamentals of Biochemistry. 2. John Wiley and Sons, Inc; 2006.

Wang CX, Song JH, Song DK, Yong VW, Shuaib A, Hao C. Cyclin-dependent kinase-5 prevents neuronal apoptosis through ERK-mediated upregulation of Bcl-2. Cell Death and Differentiation. 2006; 13:1203–12. [PubMed: 16273078]

Wu M, Neilson A, Swift AL, Moran R, Tamagnine J, Parslow D, Armistead S, Lemire K, Orrell J, Teich J, Chomicz S, Ferrick DA. Multiparameter metabolic analysis reveals a close link between attenuated mitochondrial bioenergetic function and enhanced glycolysis dependency in human tumor cells. Am J Physiol Cell Physiol. 2007; 292:C125–36. [PubMed: 16971499]

Yadava N, Nicholls DG. Spare respiratory capacity rather than oxidative stress regulates glutamate excitotoxicity after partial respiratory inhibition of mitochondrial complex I with rotenone. Journal of Neuroscience. 2007; 27:7310–7. [PubMed: 17611283]

Zhang C, Duvic M. Treatment of cutaneous T-cell lymphoma with retinoids. Dermatol Ther. 2006; 19:264–71. [PubMed: 17014481]

Highlights

- RA enhances both glycolysis and oxidative phosphorylation in SH-SY5Y cells.
- RA treatment does not increase mitochondrial number.
- RA treatment does not change the composition of the respiratory chain.
- RA treatment increases the spare respiratory capacity of mitochondria.
- Retinoic acid-induced differentiation increases the rate of oxygen consumption and enhances the spare respiratory capacity of mitochondria in SH-SY5Y cells

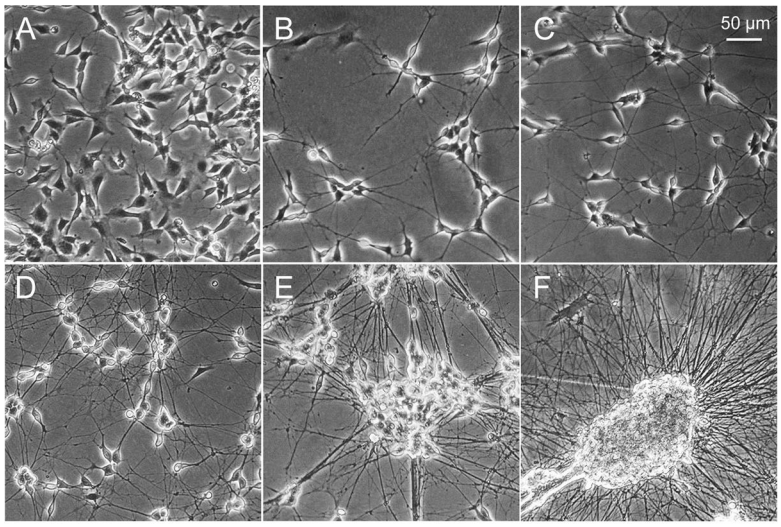

Figure 1. SH-SY5Y cells undergo morphological changes during RA-induced differentiation

(A) Undifferentiated SH-SY5Y cells cultured in complete growth medium. (B) SH-SY5Y cells treated with 10 μM RA for 4 days. SH-SY5Y cells cultured with 10 μM RA for 5 days followed by 50 ng/ml BDNF treatment for (C) 2 days, (D) 5 days, (E) 8 days, and (F) 15 days.

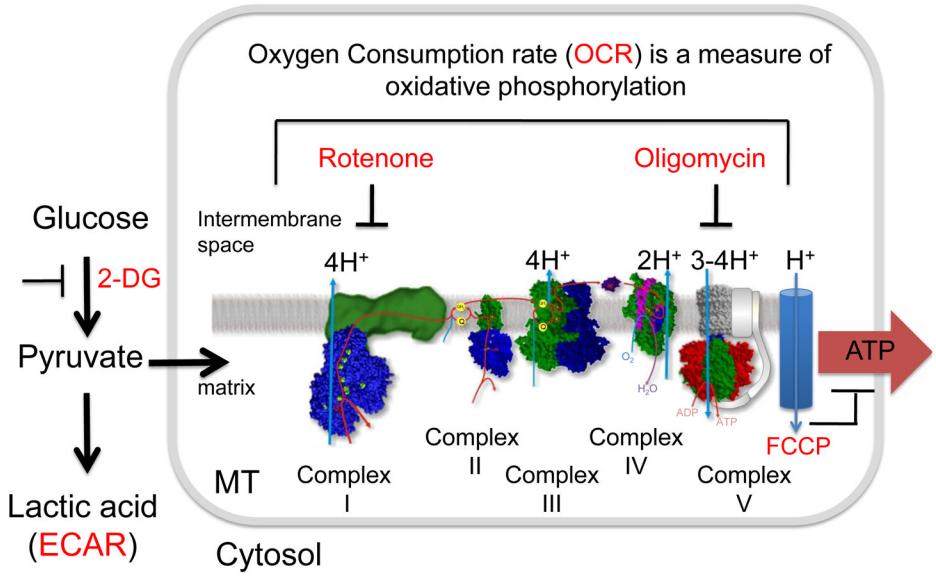

Figure 2. Simplified diagram of glycolysis and oxidative phosphorylation with corresponding pathway inhibitors

Glycolysis converts glucose to cytosolic pyruvate, which is either converted to lactic acid, measured as the extracellular acidification rate (ECAR, red), or enters the mitochondrial matrix as a substrate for oxidative phosphorylation, measured as oxygen consumption rate (OCR, red). If glycolysis is inhibited by a glucose analog, 2-deoxy-glucose (2-DG), ECAR decreases. Energy production through oxidative phosphorylation is blocked by inhibiting electron transport at any of the Complexes I, II, III, IV, and V (ATP synthase). Rotenone is an inhibitor of mitochondrial NADH dehydrogenase (complex I). Oligomycin is an inhibitor of ATP synthase (complex V). Blocking oxidative phosphorylation increases conversion of pyruvate to lactic acid, i.e., ECAR increases and OCR decreases. Electron transport generates a proton gradient (H^+) in the mitochondrial intermembrane space. These protons re-enter the matrix when ATP synthase converts ADP to ATP. FCCP is an ionophore, which allows premature reentry of the protons into the mitochondrial matrix (blue cylinder) and dissipates the proton gradient. FCCP does not inhibit electron transport, but the increase in OCR is uncoupled from ATP synthesis.

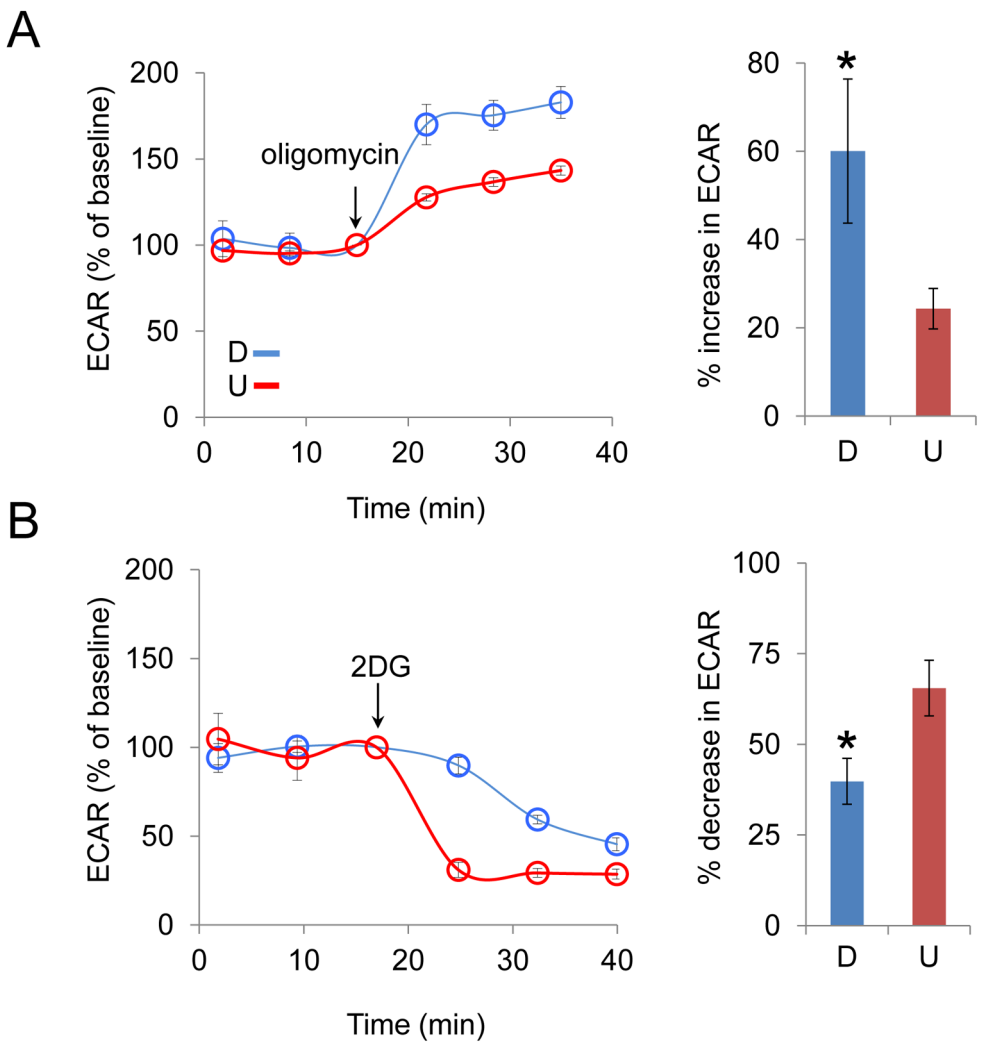

Figure 3. RA treatment reduces the dependence on glycolysis in SH-SY5Y cells

(A, left) The increase of extracellular acidification rate (ECAR) with time after oligomycin (2 μg/ml) treatment in differentiated (D, blue) and undifferentiated (U, red) cells, respectively; (A, right) The average increase in ECAR after oligomycin treatment plotted as a percent of baseline. (B, left) The decrease of ECAR with time after 2-DG (100 mM) treatment in D (blue) and U (red) cells, respectively; (B, right) The average decrease in ECAR after 2-DG treatment plotted as a percent of baseline. The % increase or decrease in ECAR was calculated as an average of the three data points after the injection of oligomycin or 2-DG. The experiments were performed with three biological replicates (three independent cultures of cells) and each point in each biological replicate was measured in triplicate. D and U denote differentiated and undifferentiated cells, respectively. ECAR was determined using a Seahorse XF96 extracellular flux analyzer. The arrow indicates the time point when the reagent was added. *, $p < 0.05$ (n = 3, Student's t-test). Error bars, SD.

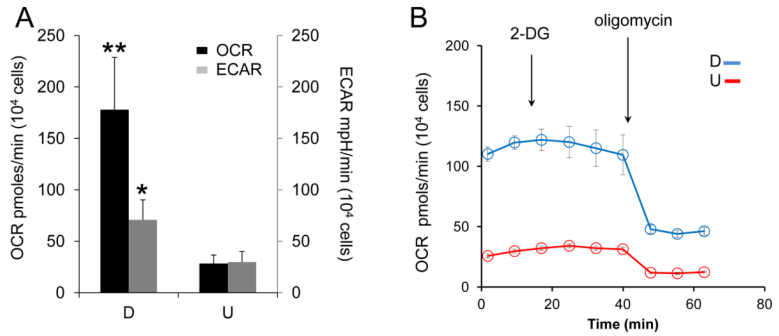

Figure 4. RA treatment increases both glycolysis and oxidative phosphorylation in SH-SY5Y cells

(A) Oxygen consumption rate (OCR, black bars, left y-axis) and extracellular acidification rate (ECAR, gray bars, right y-axis) in differentiated cells (D) are elevated relative to undifferentiated cells (U). Data shown are the average ± SD of three independent samples. Each sample was subjected to multiple measurements (n≥16) on a seahorse XF96 cell culture microplate. (B) The response of OCR with time after 2-DG (100 mM) and oligomycin (2 μg/ml) injection in D (blue) and U (red) cells, respectively. Blocking of glycolysis with 2-DG does not significantly alter the OCR values and the relative differences in OCR between D and U cells. Data shown are the average ± SEM (n = 4). OCR and ECAR were determined using a Seahorse XF96 extracellular flux analyzer. *, $p < 0.05$; **, $p < 0.01$ (n = 3, Student's t-test).

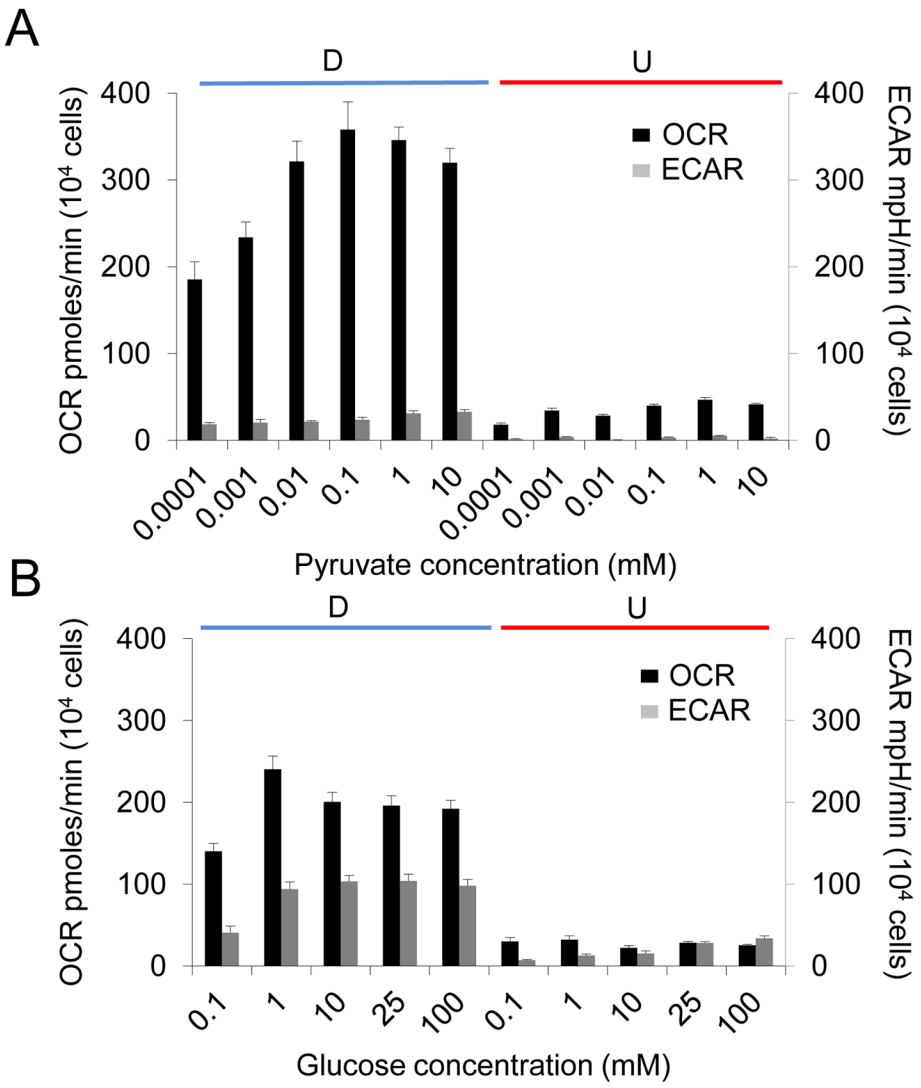

Figure 5. The metabolic feature is an emergent property of RA-induced differentiation in SH-SY5Y cells

(A) Oxygen consumption rate (OCR, black bars) and extracellular acidification rate (ECAR, gray bars) in D and U cells in response to increasing pyruvate concentrations in the absence of glucose. The pyruvate concentrations (in mM) are as indicated. (B) OCR (black bars) and ECAR (gray bars) in D and U cells in response to increasing glucose concentrations in the absence of pyruvate. The glucose concentrations (in mM) are as indicated. Saturating levels of both pyruvate and glucose did not increase OCR and ECAR in U-SH-SY5Y cells to that observed in D-SH-SY5Y cells. Data shown are the mean ± SEM, n = 6.

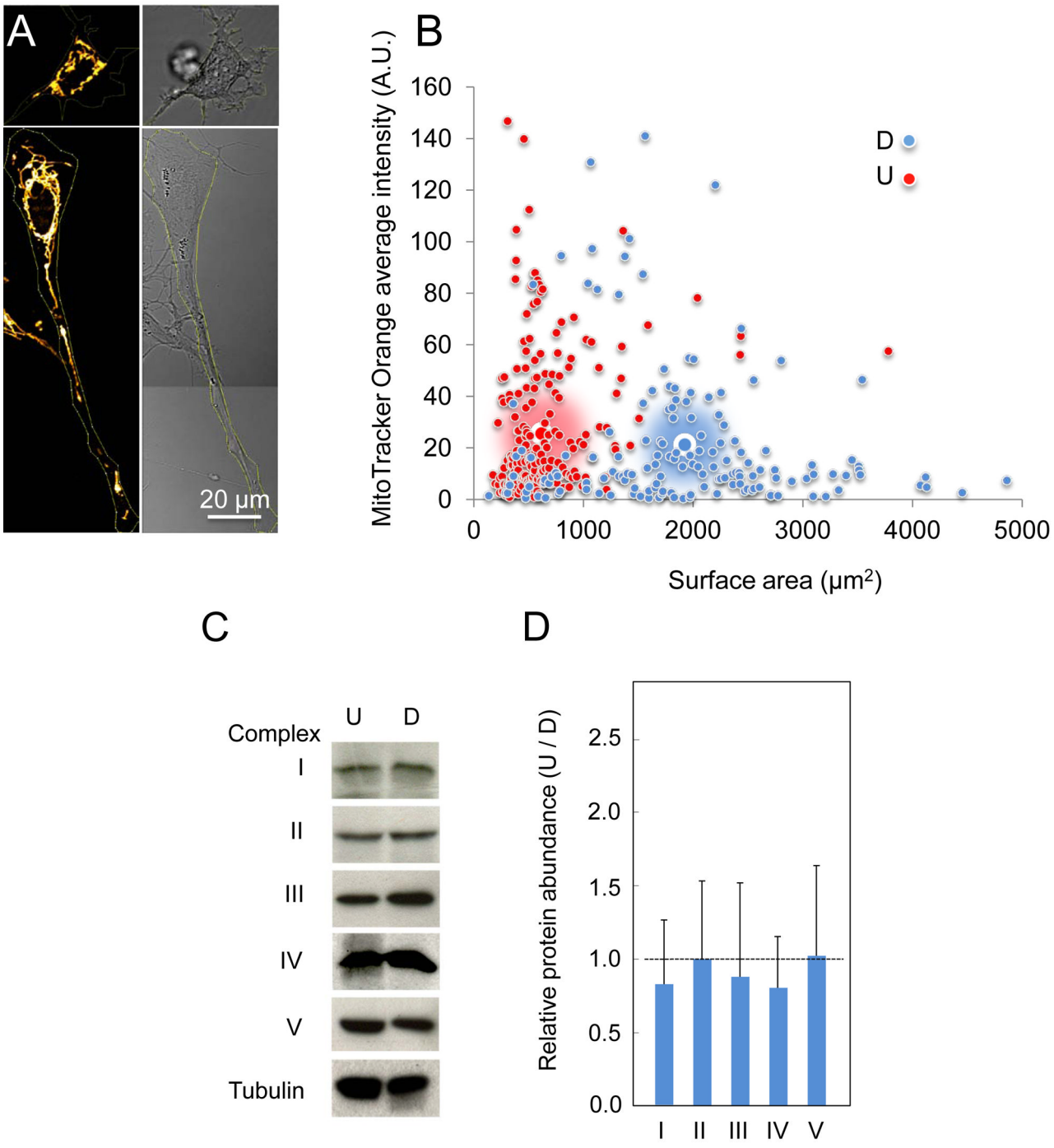

Figure 6. RA treatment does not increase the number of MT or substantially change the composition of the electron transport chain in SH-SY5Y cells

(A, left) MT of a representative undifferentiated (U) SH-SY5Y cell (top) and a representative differentiated (D) SH-SY5Y (bottom) cell visualized by MitoTracker Orange staining. (A, right) The corresponding bright-field image for A, left. (B) Plot of the average intensity of MitoTracker Orange signal versus cell surface area for D and U cells. Large blue-white circles and large red-white circles indicate the population average for D and U cells, respectively. The MitoTracker Orange intensity normalized to cell surface area is

similar between D and U cells. Scale bar is 20 microns. (C) Immunoblots of tubulin, nuclear-encoded subunits in mitochondrial complex I (NDUFB8), complex II (subunit A), complex III (subunit core 2), complex V (ATP synthase subunit beta), and MT-encoded Cytochrome C oxidase subunit II (complex IV). (D) Quantification of band densitometry normalized to the tubulin loading control. The data represent the mean ± SD of three independent measurements.

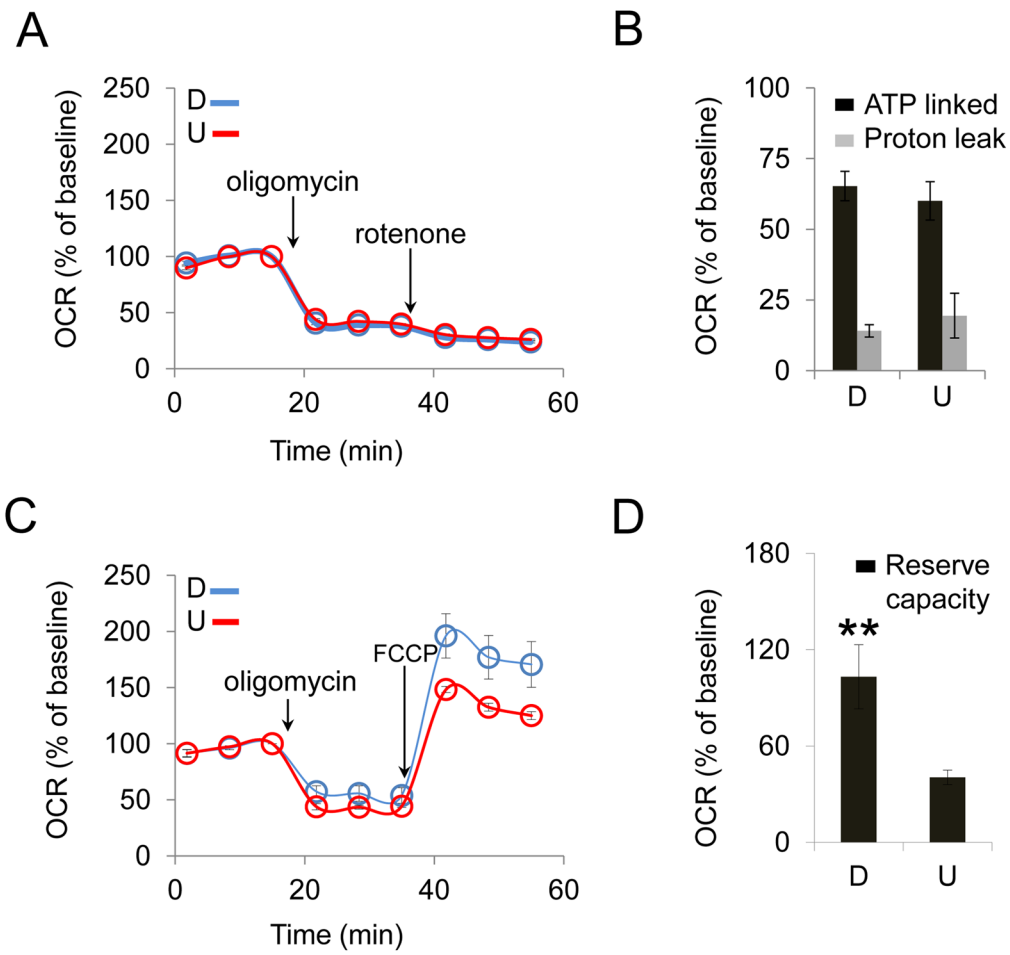

Figure 7. RA treatment increases the reserve capacity of SH-SY5Y cells

(A) Representative OCR profiles of differentiated (D) and undifferentiated (U) cells upon injection of mitochondrial inhibitor oligomycin (2 μg/ml) followed by injection of rotenone (2 μM) as a function of time. (B) ATP-linked mitochondrial respiration (black bars, obtained from the OCR decrease upon injection of oligomycin) and proton leak (gray bars, obtained from rotenone injection sequentially after oligomycin injection) did not show substantial differences between D and U cells. (C) Representative OCR profiles of D and U cells upon injection of mitochondrial inhibitors oligomycin (2 μg/ml) and mitochondrial membrane potential uncoupler FCCP (0.375 μM). (D) Reserve capacity (obtained from FCCP injection sequentially after oligomycin injection) is significantly higher in D cells than that in U cells. ** $p < 0.01$ (n = 3, Student's t-test). Error bars, SD.